

doi: 10.17586/2226-1494-2025-25-4-626-634

Spectral diagnostics of Al-Ni alloys under laser irradiation: effect of laser energy on plasma parameters

Mohammed Hamza Jawad¹✉, Mohammed Ridha Abdulameer², Kadhim Abdulwahid Aadim³

^{1,2,3} University of Baghdad, Baghdad, 00964, Iraq

¹ mohammed.hamza1204a@sc.uobaghdad.edu.iq✉, <https://orcid.org/0009-0001-8111-8195>

² mohammed_plasma@sc.uobaghdad.edu.iq, <https://orcid.org/0000-0002-7395-9840>

³ kadhim.aadim@ilps.uobaghdad.edu.iq, <https://orcid.org/0000-0003-4533-5309>

Abstract

In this research, the effect of laser beam energy on the properties and behavior of plasma produced from aluminum and nickel alloy was studied using the Optical Stimulated Emission Spectroscopy method. The properties of the plasma were characterized by exposing the target material (the alloy) to high-energy laser pulses ranging from 500 to 900 mJ using a pulsed Nd:YAG laser with a pulse rate of up to 50 Hz. This ensures a balanced energy distribution and allows monitoring of the increasing effects in the plasma without strong thermal effects. This method allows for a detailed study of the physical properties of the plasma, including the spectral radiation intensity and associated emission peak as well as the study of various plasma properties such as temperature and electron density and other plasma parameters, including the plasma frequency, Debye length, and Debye number. The results obtained show that both temperature and density increase with increasing laser power, with both effects peaking at a laser power of 900 mJ. Calculations of the plasma frequency and Debye number also show a concomitant increase in these two effects with increasing laser power. This work demonstrates how laser power can increase plasma stability and significantly improve physical processes within plasma. It also demonstrates how diagnostic techniques can be useful in plasma analysis and have numerous medical, industrial, and technological applications.

Keywords

Al-Ni alloy, optical spectroscopy of plasma, OES, plasma properties, plasma parameters

For citation: Jawad M.H., Abdulameer M.R., Aadim K.A. Spectral diagnostics of Al-Ni alloys under laser irradiation: effect of laser energy on plasma parameters. *Scientific and Technical Journal of Information Technologies, Mechanics and Optics*, 2025, vol. 25, no. 4, pp. 626–634. doi: 10.17586/2226-1494-2025-25-4-626-634

УДК 543.428

Спектральный анализ сплавов Al-Ni при лазерном облучении: влияние энергии лазера на параметры плазмы

Мохаммед Хамза Джавад¹✉, Мохаммед Ридха Абдуламир², Кадхим Абдулвахид Аадим³

^{1,2,3} Университет Багдада, Багдад, 00964, Ирак

¹ mohammed.hamza1204a@sc.uobaghdad.edu.iq✉, <https://orcid.org/0009-0001-8111-8195>

² mohammed_plasma@sc.uobaghdad.edu.iq, <https://orcid.org/0000-0002-7395-9840>

³ kadhim.aadim@ilps.uobaghdad.edu.iq, <https://orcid.org/0000-0003-4533-5309>

Аннотация

Исследованы свойства и поведение плазмы, полученной из алюминийно-никелевых сплавов при лазерном облучении. Исследование выполнено методом оптической стимулированной эмиссионной спектроскопии. Свойства плазмы модулировались путем воздействия на целевой материал (сплав) высокоэнергетическими лазерными импульсами в диапазоне энергий от 500 до 900 мДж с использованием импульсного лазера Nd:YAG при частоте импульсов до 50 Гц. Это обеспечивает сбалансированное распределение энергии и позволяет контролировать нарастающие эффекты в плазме без сильных тепловых эффектов. Примененный метод позволяет детально изучать физические свойства плазмы, включая спектральную интенсивность излучения и связанный с

© Jawad M.H., Abdulameer M.R., Aadim K.A., 2025

ней пик излучения, исследовать различные свойства плазмы, такие как электронные температура и плотность, а также другие параметры плазмы, включая плазменную частоту, длину и число Дебая. Полученные результаты показывают, что электронные температура и плотность увеличиваются с повышением мощности лазера, причем оба эффекта достигают максимума при мощности импульсов лазера 900 мДж. Расчеты плазменной частоты и числа Дебая также демонстрируют увеличение этих двух эффектов с ростом мощности импульсов лазера. Выполненное исследование показывает, что путем изменения мощности лазера можно повысить стабильность плазмы и значительно улучшить баланс физических процессов внутри плазмы. Предложенные методы исследования могут быть полезны при анализе плазмы и иметь многочисленные медицинские, промышленные и технологические приложения.

Ключевые слова

сплав Al-Ni, оптическая спектроскопия плазмы, ОЭС, свойства плазмы, параметры плазмы

Ссылка для цитирования: Джавад М.Х., Абдуламир М.Р., Аадим К.А. Спектральный анализ сплавов Al-Ni при лазерном облучении: влияние энергии лазера на параметры плазмы // Научно-технический вестник информационных технологий, механики и оптики. 2025. Т. 25, № 4. С. 626–634 (на англ. яз.). doi: 10.17586/2226-1494-2025-25-4-626-634

Introduction

Plasma can be generated by a very high temperature rise in the material to reach a stage where we can overcome the electrostatic forces that bind the material electrons to the nucleus [1]. Plasma radiation depends on the properties of the isolated radiation types and the surrounding environment around the radiation. This dependence results from the fact that electrons and ions can interact with other material due to the effect of Coulomb forces which have a long-term effect and action [2]. Plasma spectrum analysis is one of the most important methods we use to study and understand the properties of plasma used in many applications, whether in technological or industrial applications or in research such as plasma physics and space sciences where plasma can be divided based on its temperature into two types: the first is hot plasma or what is called fusion plasma, and the second type is cold plasma or gas discharge plasma [3]. If the plasma temperature drops from 300 K to 1 K, this type of plasma will be called super cold plasma. This type can be generated in a vacuum by ionizing atoms that are cooled using a laser [3].

The method of using a laser beam is considered one of the most important and popular techniques used in producing plasma. This is done by focusing a high-energy laser pulse on any material whether this material is solid, liquid, or gaseous. The resulting radiation will cause local thermal equilibrium, severe vaporization of the material and collapse of the material at the point of focus [4–6]. The interaction between matter and the laser beam will depend on a set of physical and mechanical properties as well as some chemical properties, in addition to the properties and specifications of the laser used, such as the power of the laser pulse, the focusing time, and the wavelength used [7–9].

Optical radiation analysis is one of the common methods used to examine and diagnose plasma which can provide us with important information about the sample used as well as the information about the plasma produced, as the plasma produced by laser will produce different and varied radiation spectra most of which extend between the ultraviolet region to the visible and infrared regions. This method depends on the analysis of the optical emissions generated by the plasma using a laser, which is often known as laser-induced plasma analysis or Laser-Induced Breakdown Spectroscopy (LIBS) [10, 11].

LIBS technology is used to determine the main components of the targets using conventional and non-conventional calibration methods that are considered free from calibration. Due to the need for immediate and rapid tests that determine the components of material, this method has evolved very quickly in many applications, since it is used to obtain rapid results in laboratories and the field of industry, as this can be done from long distances of up to 110 meters, and there is no need to prepare samples before starting the test [12, 13].

Spectral line broadening mechanisms such as Stark broadening detract from accurate results or reduce the quality of the spectrum in LIBS technology, as these defects can be controlled by adjusting the time and the width of the acquisition window, but they ultimately limit the acquisition of quantitative and analytical data and isotope information. Therefore, many attempts have been made to increase the accuracy of the spectrum and improve the quality of detection in the LIBS system [14]. These attempts included the repeated use of laser pulses and performing the diagnosis using more than one energy as well as the processes of improving the spectrometer angle by changing its angles to reach the best possible angle for reading the spectrum [15–18].

The main objective of this study was to investigate the laser-stimulated light emission using locally prepared 80:20 aluminum-nickel (Al-Ni) alloy to determine the general properties of the plasma generated by these alloys. This distinguishes our study from most previous studies that relied on taking the spectrum of a single element or doping a specific element with another. This alloy provides greater stability in its interaction with the plasma compared to aluminum or nickel alone, which aids in more accurate analysis and characterization because the response is somewhat more diverse when exposed to laser pulses. Fig. 1 shows a cross-section of the alloy used.

Materials and methodology

Preparing an Al-Ni Alloy for Laser Blasting

An Al-Ni alloy was locally prepared with a composition ratio of 80:20 using a gas furnace to ensure optimal homogeneity of the constituent material. The purity of the elements from which the alloy was made reached 98 %. A sample of this alloy 2 cm² and 4 mm thick was taken and



Fig. 1. Al-Ni alloy

placed on the laser base holder where it was prepared for the ablation process.

Experimental LIPS setup

Fig. 2 shows a schematic diagram of the LIBS system used in this experiment. A pulsed Nd:YAG laser with a frequency of 6 kHz and a wavelength of 1064 nm was used. Different laser energies (500 to 900 mJ) and pulse rates of up to 50 Hz were used. The sample was placed on a metal support surface, and the laser was focused at a 45° angle to initiate the ablation process. The resulting optical data were then collected using a Surwit S3000-UV-NIR spectrometer which is characterized by its rapid response to changes in emitted radiation and operates in the ultraviolet, infrared, and visible light ranges across the wavelength range of 200 to 1000 nm. These spectra were recorded on a control unit (PC) to initiate the analysis and data extraction process.

Results and Discussion

The plasma produced by the Al-Ni alloy was characterized using stimulated photoemission spectroscopy. The emission spectrum of this alloy plasma consists of optical radiation resulting from the decay of excited elements within the plasma, and the spectrum is often

presented in the form of spectral lines characteristic of atoms or ions. The spectral range for the alloy used ranged from 200 nm to 800 nm for most of its constituent elements. The emission peaks for all elements were compared with data from the National Institute of Standards and Technology (NIST)¹.

Fig. 3 shows that there are several emission peaks for the elements that make up the Al-Ni alloy. Aluminum emitted at wavelengths of 235.5, 256.5, 280.5, 308.2, 324.1, 345.2, 465.3, and 521 nm, while nickel emitted at wavelengths of 357.7, 394.6, 452.3, 485.5, 514.6, and 546.8 nm. On the other hand, we saw several peaks for nitrogen emission, the most prominent of which was at a wavelength of 623.8 nm, as well as several peaks for oxygen, the most prominent of which was at a wavelength of 0.2 nm.

It was noted, as shown in the Fig. 3, that the intensity of the emission of spectral lines will increase with the increase in the energy of the laser used, as the main reason for this is because of the rise in the removal of electrons caused by the laser energy during the process of ionization of the elements which increased the production of ions [19]. These results show that the behavior of Al-Ni alloy plasma differs from that of pure material such as aluminum and nickel alone, as the complex composition of the alloy affects the intensity of the spectral emissions and the ratio between aluminum and nickel, indicating the presence of complex interconnected excitation and ionization processes within the plasma. The nickel to aluminum ratio changed with laser energies, showing that nickel is strongly ionized despite its small proportion in the alloy composition. This is due to the difference in ionization energies and the properties of energy transfer between atoms within the produced plasma. The Al-Ni emission intensity ratios were calculated at different laser energies and found to be approximately 1.22 at 500 mJ, 1.21 at

¹ NIST Atomic Spectra Database Lines Form. Available at: <https://www.nist.gov/pml/atomic-spectra-database>, free. English lang. (accessed: 15.07.2025).

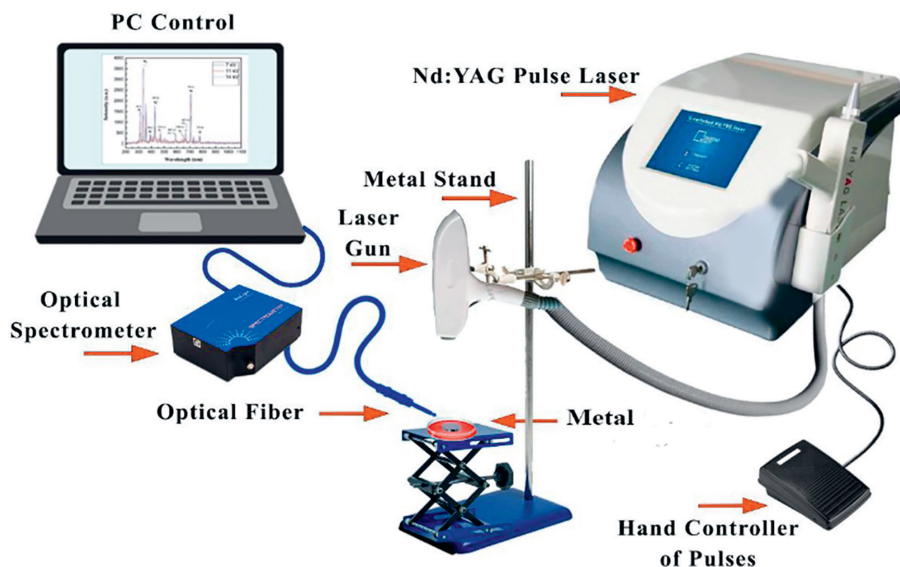


Fig. 2. Basic components of an induced laser spectroscopy system

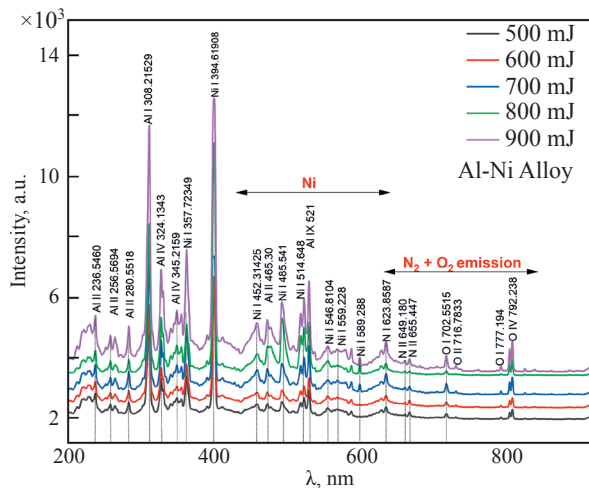


Fig. 3. Plasma emission spectrum for an Al-Ni target at different laser intensity

600 mJ, 1.03 at 700 mJ, 1.37 at 800 mJ, and 1.09 at 900 mJ. These values were close to unity, indicating that nickel, despite its lower proportion in the alloy exhibited emissions like, or sometimes higher than, aluminum. The physical reason for this is the difference in ionization energies and energy transfer probabilities between the two elements. Aluminum has lower ionization energy and therefore ionizes more easily, while nickel produces more intense lines due to the higher transfer probabilities for some of its lines. Furthermore, the alloy composition played an important role in plasma formation because of the presence of more than one element created a complex plasma environment that affected the excitation and ionization processes, causing varying emission ratios. These results confirmed that the alloy was not merely a mixture but rather an interconnected plasma environment, which makes the plasma behave differently from pure metals. Thus, these ratios are an important indicator for understanding the interaction of elements in plasma and improving the accuracy of LIBS analysis. The results of this study are compared with previous studies that addressed plasma behavior in pure metals and some alloy using LIBS. For example, Hanif et al. [20] analyzed nickel plasma using an Nd:YAG laser, showing the effect of laser parameters on plasma properties such as electron temperature and electron density. Another study by Ahmed et al. [21] compared copper-nickel alloy using multiple techniques, such as LIBS, LA-TOF, EDX, and XRF, demonstrating the importance of using multiple techniques to accurately analyze alloy. Compared to these studies, our research highlights the advantages of LIBS analysis of Al-Ni

alloy contributing to improved analytical accuracy and understanding of plasma behavior in alloy compared to pure metals [22].

The Boltzmann diagram method was used to calculate the electron temperature in the plasma produced by an Al-Ni alloy after exposing it to a laser beam. Specific wavelengths from the resulting spectrum were used for this purpose: 357.72349 nm, 394.61908 nm, 452.31425 nm, 485.541 nm, and 546.8104 nm, which are due to the emission of nickel, according to the data shown in the Table 1.

In Table 1, A_G refers to the Einstein coefficient for spontaneous emission, which represents the transition probability of an excited electron decaying to a lower energy level expressed in units of s^{-1} .

This process involved extracting the electron energy E_j for each wavelength by comparing the spectrum data with the NIST database. Energy data for each wavelength were obtained to apply them to the Boltzmann equation below to calculate the electron temperature in the plasma [23].

$$\ln \left[\frac{\lambda_{ji} I_{ji}}{hc A_{ji} g_j} \right] = \frac{1}{k_B T} (E_j) + \ln N/U(T). \quad (1)$$

Eq. (1) shows the dependence of $\ln(\lambda_{ji} I_{ji}/A_{ji} g_j)$ versus E_j , where λ_{ji} represents the radiation intensity at wavelength λ_j ; E_j is the maximum energy associated with this wavelength; h Planck's constant; c is the speed of light in a vacuum; k_B is the Boltzmann constant, which is used in thermodynamic energy equations; T represents the absolute temperature of the substance being measured; N stands for the number of molecules or atoms in the system; U is the internal energy of the system at temperature T . I_{ji} represents the intensity of the spectral line corresponding to the transition from the upper-level j to the lower level i ; A_{ji} is the Einstein coefficient for spontaneous emission associated with this transition expressed in s^{-1} ; and g_j is the statistical weight (degeneracy) of the upper energy level j .

When the relationship between the variables is plotted, the resulting slope represents the relationship $1/k_B T$, which was used to calculate the electron temperature. The results obtained through this analysis showed that the electron temperature increases significantly with increasing laser beam energy. The highest temperature reached by the electrons was 0.726 eV at a laser energy of 900 mJ. The closer its value is to one, the higher the accuracy.

Fig. 4 shows the results of the Boltzmann plot between $\ln(\lambda_{ji} I_{ji}/A_{ji} g_j)$ versus E_j for different energies used. R^2 represents the correlation coefficient which reflects the accuracy of the graph and the correlation of the points with each other.

One of the most important and common methods for calculating electron density is the Stark exposure measurement which is calculated from the width of a single spectral line of an atom or ion. This effect is a direct result of the collision of charged particles and atoms. This effect is a physical phenomenon that occurs when a charged gas is exposed to an external electric field. Due to this interaction, the movement of electrons will change, thus causing a broadening of the spectral lines, which directly affects the electron density. The relationship between density and

Table 1. Basic parameters of Al-Ni Alloy plasma

Element	λ_{NIST} , nm	A_G , s^{-1}	E_j , eV
Ni	357.72349	$8.00 \cdot 10^4$	3.739751
	394.61908	$1.50 \cdot 10^3$	3.306149
	452.31425	$2.90 \cdot 10^0$	2.740339
	485.54100	$2.80 \cdot 10^8$	6.094943
	546.81040	$5.50 \cdot 10^6$	6.114134

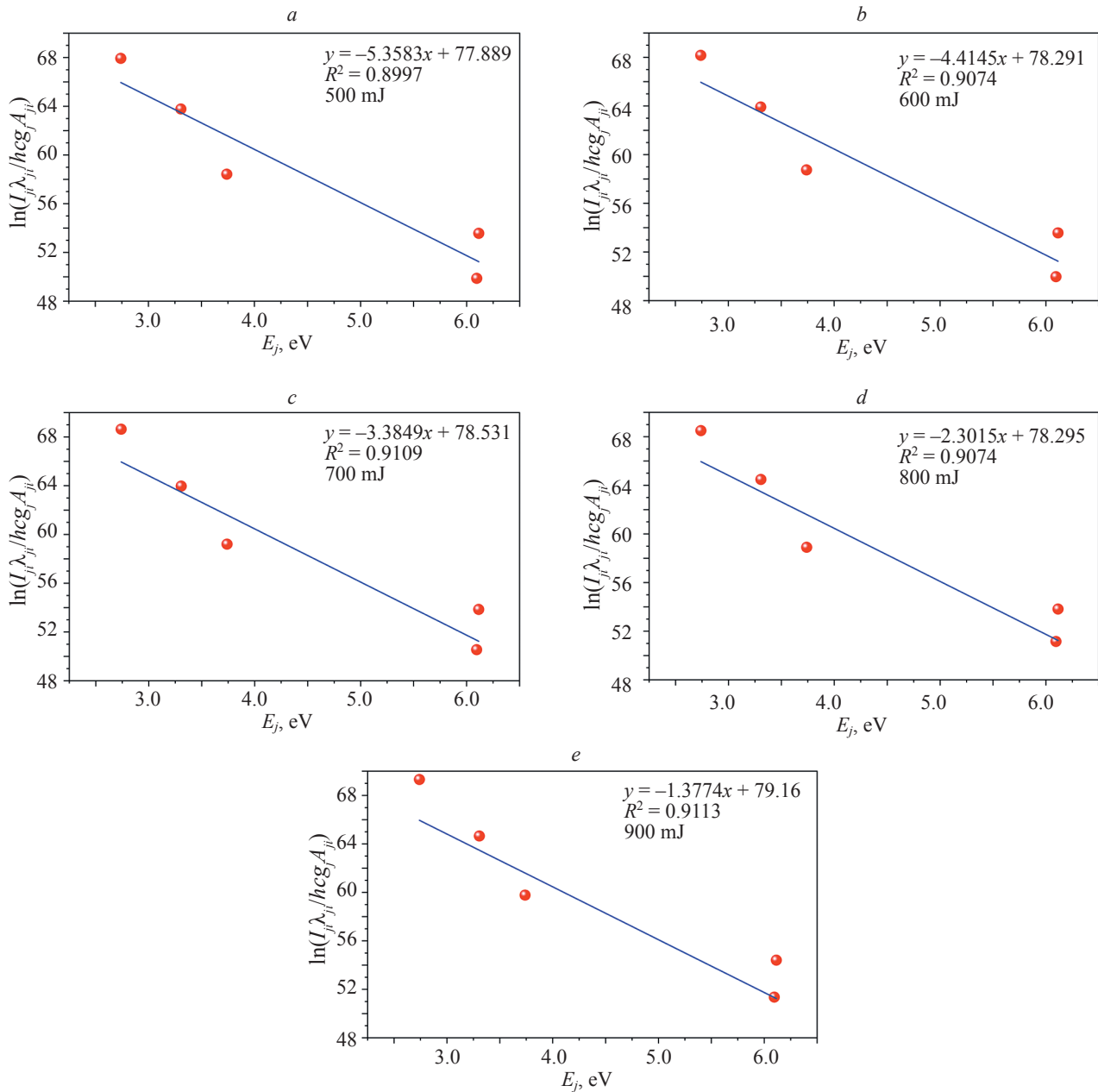


Fig. 4. Boltzmann diagrams for the Al-Ni alloy at energies, mJ: 500 (a), 600 (b), 700 (c), 800 (d), 900 (e)

spectral line width is a direct relationship. This can be expressed mathematically using equation from [23]:

$$n_e(\text{cm}^{-3}) = \left(\frac{\Delta\lambda_{\text{FWHM}}}{2w} \right) \cdot 10^{17}. \quad (2)$$

This equation represents the dependence of electron density n_e on the Full Width at Half Maximum (FWHM) ($\Delta\lambda_{\text{FWHM}}$), where $\Delta\lambda_{\text{FWHM}}$ stands for the spectral line width at half its maximum intensity, and w represents the width of the line at its minimum intensity. The full width at mid-intensity of the alloy is represented by Fig. 5, which represents the calculated exposure for the electron density (2) for the wavelength 394 nm. The electron density has risen gradually with the escalation in the laser energy employed, where it was equal to $(4.01 \cdot 10^{17} \text{ cm}^{-3})$ for an energy of 500 mJ, while it reached its peak at an energy

of 900 mJ, where it was equal to $(6.13 \cdot 10^{17} \text{ cm}^{-3})$. This increase is attributed to the absorption of the photon energy of the laser beam by the electrons, which is what is shown to us through the drawing, where we notice the change in the Stark resonance value with the change in the energy value of the laser used.

Stark broadening is related to how an external electric field affects the emission lines produced by plasma. When plasma is exposed to an external electric field, changes will occur in the emission lines. These changes cause a broadening of the line FWHM. This broadening depends directly on the electron density in the plasma, and thus, the Stark broadening will increase as the electron density increases.

As expected and mentioned, the temperature and density of the electrons will increase with increasing laser

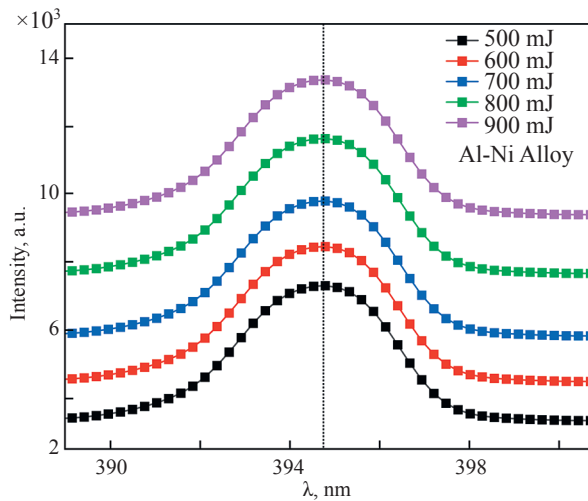


Fig. 5. Stark exposure of Al-Ni alloy

power, since this increase occurs as a result of the power of the laser having a powerful and straightforward impact on the emission lines intensity, as the value of the temperature and density of the electrons will become almost stable because the plasma will become dependent on the laser beam covering the target, and plasma shadowing occurs when the plasma itself reduces the transmission of laser energy along the beam path. Fig. 6 represents the increase and the clear difference between the density of the electrons and their temperature. These findings concur with those of Kison V.E et al. [24].

The behavior of plasma emitted by Al-Ni alloys is significantly different from that of pure metals such as aluminum or nickel alone, because the alloy composition is complex and comprises multiple elements. The presence of nickel and aluminum together creates plasma environment that differs from that of pure material as the atoms and ions interact and overlap more strongly, significantly affecting the emission spectrum. Due to the composition, the energy distribution within the plasma changes, which is reflected in the electron temperature and electron density and alters the mode of ionization and excitation. When we observe the ratio of nickel to aluminum intensities and observe their change with laser power, we realize that

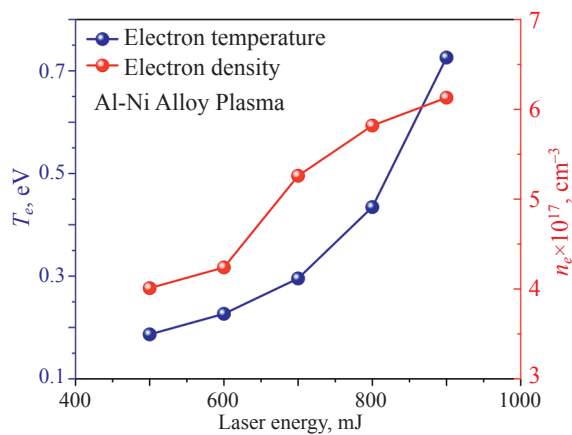


Fig. 6. Change in electron temperature T_e and density n_e as a function of laser energy

plasma behavior in alloys is more dynamic and variable than in pure metals. Therefore, it is important to study plasmas in alloy separately, as this understanding helps us improve the accuracy of LIBS analysis and advances industrial applications that rely on the analysis of composite material [24].

The effect of laser energy on some other plasma parameters, such as plasma frequency, Debye length, and the number of charged particles in the Debye sphere, is investigated using the main plasma parameters, which are electron density and temperature, to increase and improve the diagnosis of the plasma produced by the aluminum and nickel alloy where the Debye length λ_D is calculated from the equation [23]:

$$\lambda_D = \left[\frac{\epsilon_0 k_B T_e}{n_e e^2} \right]^{1/2} \cong 7.43 \times 10^2 \left(\frac{T_e}{n_e} \right)^{1/2}, \quad (3)$$

where T_e is the electron temperature; e is the elementary charge (the charge of a single electron), which is approximately $1.602 \cdot 10^{-19}$ C; n_e is the electron density, which is defined in equation (2) as the number of electrons per cubic centimeter; ϵ_0 is the permittivity of free space.

The following formula can be used to determine the plasma frequency f_p [23]:

$$f_p = \sqrt{\frac{e^2 n_e}{\epsilon_0 m_e}}, \quad (4)$$

where m_e is the electron mass, which is approximately $9.11 \cdot 10^{-31}$ kg.

The number of charged particles N_D in the Debye sphere can be calculated from the equation in [23]:

$$N_D = 4/3 \lambda_D^3 n_e. \quad (5)$$

Table 2 shows the data obtained for all plasma parameters formed from the Al-Ni alloy and for all laser energies used.

Fig. 7 shows the relationship and change in the value of plasma frequency and the relationship between laser beam energy and Debye length. The plasma frequency shows a significant increase with increasing energy, where the frequency value ranges from $5.7 \cdot 10^{12}$ to $7.0 \cdot 10^{12}$ Hz, while

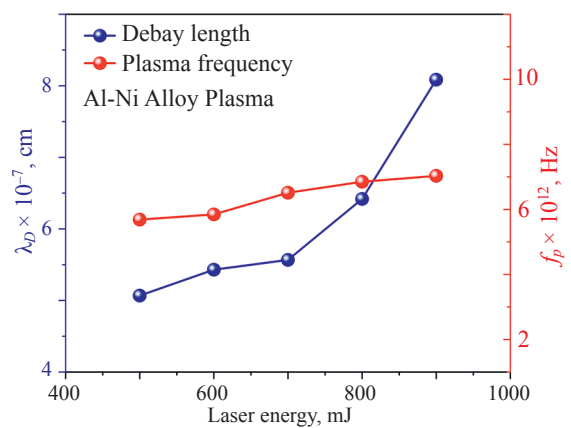


Fig. 7. Variation of plasma density f_p and Debye length λ_D as a function of laser power

Table 2. Main parameters of Al-Ni alloy plasma generated under the action of the laser beam with different values

E , mJ	T_e , eV	$n_e \times 10^{17}$, cm ⁻³	$f_p \times 10^{12}$, Hz	$\lambda_D \times 10^{-7}$, cm	$N_D \times 10^3$
500	0.187	4.01	5.7	5.1	0.21863
600	0.227	4.24	5.8	5.4	0.28433
700	0.295	5.26	6.5	5.6	0.38020
800	0.434	5.82	6.9	6.4	0.64469
900	0.726	6.13	7.0	8.1	1.35679

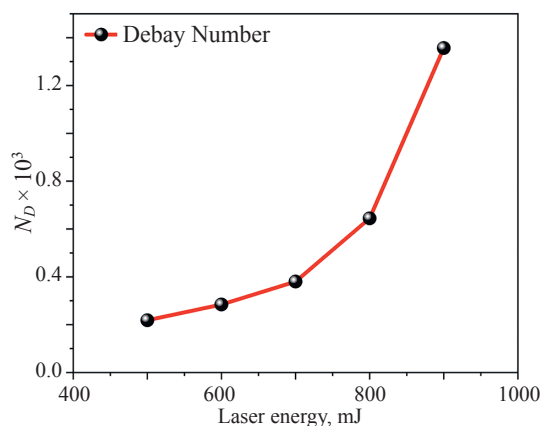


Fig. 8. Debye Number as a function of laser power

on the other hand, the Debye length will gradually decrease, where its value ranges from $5.1 \cdot 10^{-7}$ to $8.1 \cdot 10^{-7}$ cm. This is due to Eqs. (3) and (4), where the frequency corresponds exactly to the electron density, while the Debye length value is inversely proportional to the electron density. These results are consistent with Aadim K.A. et al. [25].

The Debye length increases with increasing laser power. This increase can be explained scientifically by the fact that increasing laser power increases the energy content of the plasma system, leading to the ionization of more atoms and the production of more charged particles. This is also due to the change in the electron density, which increases with increasing energy. Fig. 8 shows the relationship between the Debye length calculated using Eq. (5) and laser power.

References

1. Abdellatif G., Imam H. A study of the laser plasma parameters at different laser wavelengths. *Spectrochimica Acta Part B: Atomic Spectroscopy*, 2002, vol. 57, no. 7, pp. 1155–1165. [https://doi.org/10.1016/S0584-8547\(02\)00057-5](https://doi.org/10.1016/S0584-8547(02)00057-5)
2. Tchernycheva M.V., Marek V.P., Chirtsov A.S., Shvager D.A. Computational modeling in the study of glow discharge physical processes in the air at low pressures. *Scientific and Technical Journal of Information Technologies, Mechanics and Optics*, 2014, vol. 14, no. 3, pp. 140–148. (in Russian)
3. Jawad M.H., Abdulameer M.R. The effect of background argon gas pressure on the parameters of plasma produced by DC-glow discharge. *Iraqi Journal of Science*, 2023, vol. 64, no. 3, pp. 1210–1218. <https://doi.org/10.24996/ij.s.2023.64.3.17>
4. Baskевичius A., Balachninaite O., Karpavicius M., Butkus S., Paipulas D., Sirutkaitis V. Monitoring of the femtosecond laser micromachining process of materials immersed in water by use of

Conclusion

This work investigated the effect of laser energy on the behavior of the generated plasma using a locally manufactured aluminum-nickel alloy with a composition ratio of 80:20. The results showed that the spectral emission intensity increased with increasing laser energy. The aluminum emission peak was at a wavelength of 394.6 nm at the energy of 900 mJ, while the nickel emission peak was at 357.7 nm at the same energy. These changes indicate strong interactions between the laser beam energy and the generated plasma, leading to an overall improvement in the plasma properties. Furthermore, a clear increase in both the electron density and electron temperature was observed with increasing laser energy. The highest value of the electron temperature was at 900 mJ, which was equal to 0.726 eV, while the electron density at the same energy was $6.13 \cdot 10^{17}$ cm⁻³. This is clear evidence that the plasma electrons interact more strongly with the laser energy. The fundamental plasma parameters were also investigated to provide a further understanding of its behavior. These findings support previous studies on the subject and confirm the close relationship between plasma parameters and the applied laser power. Based on these results, we can conclude that there is a close and direct relationship between laser beam energy and plasma composition and characterization. This relationship will open new horizons and better future technologies in many industrial and technological applications and other fields, such as material analysis using Laser-Induced Breakdown Analysis. The current study also contributes to expanding scientific understanding of the mechanism of laser interaction and the effect of laser energy on plasma.

Литература

1. Abdellatif G., Imam H. A study of the laser plasma parameters at different laser wavelengths // *Spectrochimica Acta Part B: Atomic Spectroscopy*. 2002. V. 57. N 7. P. 1155–1165. [https://doi.org/10.1016/S0584-8547\(02\)00057-5](https://doi.org/10.1016/S0584-8547(02)00057-5)
2. Чернышева М.В., Марек В.П., Чирцов А.С., Швагер Д.А. Компьютерное моделирование при изучении физических процессов в тлеющем разряде в воздушной смеси при низких давлениях // *Научно-технический вестник информационных технологий, механики и оптики*. 2014. Т. 14, № 3. С. 140–148.
3. Jawad M.H., Abdulameer M.R. The effect of background argon gas pressure on the parameters of plasma produced by DC-glow discharge // *Iraqi Journal of Science*. 2023. V. 64. N 3. P. 1210–1218. <https://doi.org/10.24996/ij.s.2023.64.3.17>
4. Baskевичius A., Balachninaite O., Karpavicius M., Butkus S., Paipulas D., Sirutkaitis V. Monitoring of the femtosecond laser micromachining process of materials immersed in water by use of

- laser-induced breakdown spectroscopy. *Journal of Laser Micro/Nanoengineering*, 2016, vol. 11, no. 3, pp. 381–387. <https://doi.org/10.2961/jlmn.2016.03.0018>
5. Heidari A.A., Seyfi P., Khademi A., Ghomi H. Investigation of the effects of pulse repetition frequency in a mixed electric field on a SDBD-like plasma jet. *Journal of Theoretical and Applied Physics*, 2022, vol. 16, no. 1, pp. 162208.
6. Veiko V.P., Skvortsov A.M., Tu H.C., Petrov A.A. Laser ablation of monocrystalline silicon under pulsed-frequency fiber laser. *Scientific and Technical Journal of Information Technologies, Mechanics and Optics*, 2015, vol. 15, no. 3, pp. 426–434. (in Russian)
7. Aadim K.A. Spectroscopic study the plasma parameters for Pb doped CuO prepared by pulse Nd:YAG laser deposition. *Iraqi Journal of Physics*, 2018, vol. 16, no. 38, pp. 1–9. <https://doi.org/10.30723/ijp.v16i38.3>
8. Rashid T.M., Rahmah M.I., Mahmood W.K., Fahem M.Q., Jabir M.S., Bidan A.K., Adbalrazaq S., Jawad M.H., Awaid D.M., Qamandar M.A., Alsaffar S.M. Eco-friendly Laser Ablation for Synthesis of CNF@Au Nanoparticles: insights into enhancing NO₂ gas detection and antibacterial activity. *Plasmonics*, 2025, in press. <https://doi.org/10.1007/s11468-025-02874-z>
9. Gondal M.A., Dastageer M.A. Elemental analysis of soils by laser-induced breakdown spectroscopy. *Springer Series in Optical Sciences*, 2014, vol. 182, pp. 293–308. https://doi.org/10.1007/978-3-642-45085-3_11
10. Jawad M.H., Abdulameer M.R. Study the effect of external voltage on some plasma parameters produced by DC glow xenon gas discharge. *AIP Conference Proceedings*, 2024, vol. 2922, no. 1, pp. 150003. <https://doi.org/10.1063/5.0183126>
11. Guseva V.E., Nechay A.N., Perekalov A.A., Salashchenko N.N., Chkhalo N.I. Investigation of emission spectra of plasma generated by laser pulses on Xe gas-jet targets. *Applied Physics B*, 2023, vol. 129, no. 10, pp. 155. <https://doi.org/10.1007/s00340-023-08095-8>
12. Abbas Z.M., Abbas Q.A. Characterization of magnetized-plasma system induced by laser. *Iraqi Journal of Physics*, 2023, vol. 21, no. 4, pp. 45–55. <https://doi.org/10.30723/ijp.v21i4.1148>
13. Jawad M.H., Assi A.A., Hameed A.M. Hydrothermal synthesis of Zinc Oxide nanostructures using varied reactor designs: a comparative study. *Plasmonics*, 2025, in press. <https://doi.org/10.1007/s11468-025-02828>
14. Jha V.K., Mishra L.N., Narayan B. Impact of silica seeding and discharge voltage on plasma parameters at atmospheric pressure. *Journal of Theoretical and Applied Physics*, 2022, vol. 16, no. 1, pp. 162205
15. Phillips K.C., Gandhi H.H., Mazur E., Sundaram S.K. Ultrafast laser processing of materials: a review. *Advances in Optics and Photonics*, 2015, vol. 7, no. 4, pp. 684–712. <https://doi.org/10.1364/AOP.7.000684>
16. Aquino F.W.B., Pereira-Filho E.R. Analysis of the polymeric fractions of scrap from mobile phones using laser-induced breakdown spectroscopy: Chemometric applications for better data interpretation. *Talanta*, 2015, vol. 134, pp. 65–73. <https://doi.org/10.1016/j.talanta.2014.10.051>
17. Castro J.P., Pereira-Filho E.R. Twelve different types of data normalization for the proposition of classification, univariate and multivariate regression models for the direct analyses of alloys by laser-induced breakdown spectroscopy (LIBS). *Journal of Analytical Atomic Spectrometry*, 2016, vol. 31, no. 10, pp. 2005–2014. <https://doi.org/10.1039/C6JA00224B>
18. de M. Franco M.A., Milori D.M.B.P., Boas P.R.V. Comparison of algorithms for baseline correction of LIBS spectra for quantifying total carbon in Brazilian soils. *arXiv*, 2018, arXiv:1805.03695. <https://doi.org/10.48550/arXiv.1805>
19. Fikry M., Tawfik W., Omar M.M. Investigation on the effects of laser parameters on the plasma profile of copper using picosecond laser induced plasma spectroscopy. *Optical and Quantum Electronics*, 2020, vol. 52, no. 5, pp. 249. <https://doi.org/10.1007/s11082-020-02381-x>
20. Hanif M., Salik M., Baig M.A. Diagnostic study of nickel plasma produced by fundamental (1064 nm) and second harmonics (532 nm) of an Nd: YAG laser. *Journal of Modern Physics*, 2012, vol. 3, no. 10A, pp. 1663–1669. <https://doi.org/10.4236/jmp.2012.330203>
21. Ahmed N., Ahmed R., Rafique M., Baig M.A. A comparative study of Cu–Ni alloy using LIBS, LA-TOF, EDX, and XRF. *Laser and Particle Beams*, 2017, vol. 35, no. 1, pp. 1–9. <https://doi.org/10.1017/s0263034616000732>
- laser-induced breakdown spectroscopy // *Journal of Laser Micro/Nanoengineering*. 2016. V. 11. N 3. P. 381–387. <https://doi.org/10.2961/jlmn.2016.03.0018>
5. Heidari A.A., Seyfi P., Khademi A., Ghomi H. Investigation of the effects of pulse repetition frequency in a mixed electric field on a SDBD-like plasma jet // *Journal of Theoretical and Applied Physics*. 2022. V. 16. N 1. P. 162208.
6. Вейко В.П., Скворцов А.М., Ту Х.К., Петров А.А. Лазерная абляция монокристаллического кремния под действием импульсно-частотного излучения волоконного лазера // *Научно-технический вестник информационных технологий, механики и оптики*. 2015. Т. 15. № 3. С. 426–434.
7. Aadim K.A. Spectroscopic study the plasma parameters for Pb doped CuO prepared by pulse Nd:YAG laser deposition // *Iraqi Journal of Physics*. 2018. V. 16. N 38. P. 1–9. <https://doi.org/10.30723/ijp.v16i38.3>
8. Rashid T.M., Rahmah M.I., Mahmood W.K., Fahem M.Q., Jabir M.S., Bidan A.K., Adbalrazaq S., Jawad M.H., Awaid D.M., Qamandar M.A., Alsaffar S.M. Eco-friendly Laser Ablation for Synthesis of CNF@Au Nanoparticles: insights into enhancing NO₂ gas detection and antibacterial activity // *Plasmonics*. 2025. in press. <https://doi.org/10.1007/s11468-025-02874-z>
9. Gondal M.A., Dastageer M.A. Elemental analysis of soils by laser-induced breakdown spectroscopy // *Springer Series in Optical Sciences*. 2014. V. 182. P. 293–308. https://doi.org/10.1007/978-3-642-45085-3_11
10. Jawad M.H., Abdulameer M.R. Study the effect of external voltage on some plasma parameters produced by DC glow xenon gas discharge // *AIP Conference Proceedings*. 2024. V. 2922. N 1. P. 150003. <https://doi.org/10.1063/5.0183126>
11. Guseva V.E., Nechay A.N., Perekalov A.A., Salashchenko N.N., Chkhalo N.I. Investigation of emission spectra of plasma generated by laser pulses on Xe gas-jet targets // *Applied Physics B*. 2023. V. 129. N 10. P. 155. <https://doi.org/10.1007/s00340-023-08095-8>
12. Abbas Z.M., Abbas Q.A. Characterization of magnetized-plasma system induced by laser // *Iraqi Journal of Physics*. 2023. V. 21. N 4. P. 45–55. <https://doi.org/10.30723/ijp.v21i4.1148>
13. Jawad M.H., Assi A.A., Hameed A.M. Hydrothermal synthesis of Zinc Oxide nanostructures using varied reactor designs: a comparative study // *Plasmonics*. 2025. in press. <https://doi.org/10.1007/s11468-025-02828-5>
14. Jha V.K., Mishra L.N., Narayan B. Impact of silica seeding and discharge voltage on plasma parameters at atmospheric pressure // *Journal of Theoretical and Applied Physics*. 2022. V. 16. N 1. P. 162205
15. Phillips K.C., Gandhi H.H., Mazur E., Sundaram S.K. Ultrafast laser processing of materials: a review // *Advances in Optics and Photonics*. 2015. V. 7. N 4. P. 684–712. <https://doi.org/10.1364/AOP.7.000684>
16. Aquino F.W.B., Pereira-Filho E.R. Analysis of the polymeric fractions of scrap from mobile phones using laser-induced breakdown spectroscopy: Chemometric applications for better data interpretation // *Talanta*. 2015. V. 134. P. 65–73. <https://doi.org/10.1016/j.talanta.2014.10.051>
17. Castro J.P., Pereira-Filho E.R. Twelve different types of data normalization for the proposition of classification, univariate and multivariate regression models for the direct analyses of alloys by laser-induced breakdown spectroscopy (LIBS) // *Journal of Analytical Atomic Spectrometry*. 2016. V. 31. N 10. P. 2005–2014. <https://doi.org/10.1039/C6JA00224B>
18. de M. Franco M.A., Milori D.M.B.P., Boas P.R.V. Comparison of algorithms for baseline correction of LIBS spectra for quantifying total carbon in Brazilian soils // *arXiv*. 2018. arXiv:1805.03695. <https://doi.org/10.48550/arXiv.1805>
19. Fikry M., Tawfik W., Omar M.M. Investigation on the effects of laser parameters on the plasma profile of copper using picosecond laser induced plasma spectroscopy // *Optical and Quantum Electronics*. 2020. V. 52. N 5. P. 249. <https://doi.org/10.1007/s11082-020-02381-x>
20. Hanif M., Salik M., Baig M.A. Diagnostic study of nickel plasma produced by fundamental (1064 nm) and second harmonics (532 nm) of an Nd:YAG laser // *Journal of Modern Physics*. 2012. V. 3. N 10A. P. 1663–1669. <https://doi.org/10.4236/jmp.2012.330203>
21. Ahmed N., Ahmed R., Rafique M., Baig M.A. A comparative study of Cu–Ni alloy using LIBS, LA-TOF, EDX, and XRF // *Laser and Particle Beams*. 2017. V. 35. N 1. P. 1–9. <https://doi.org/10.1017/s0263034616000732>

22. Lober R., Mazumder J. Spectroscopic diagnostics of plasma during laser processing of aluminium. *Journal of Physics D: Applied Physics*, 2007, vol. 40, no. 19, pp. 5917. <https://doi.org/10.1088/0022-3727/40/19/021>
23. Shehab M.M., Aadim K.A. Spectroscopic diagnosis of the CdO: CoO plasma produced by Nd:YAG laser. *Iraqi Journal of Science*, 2021, vol. 62, no. 9, pp. 2948–2955. <https://doi.org/10.24996/ijis.2021.62.9.11>
24. Kison V.E., Mustafaev A.S., Sukhomlinov V.S. Development of a new plasma technology for producing pure white corundum. *Scientific and Technical Journal of Information Technologies, Mechanics and Optics*, 2021, vol. 21, no. 3, pp. 380–385. (in Russian). <https://doi.org/10.17586/2226-1494-2021-21-3-380-385>
25. Aadim K.A., Ahmed B.M., Khalaf M.A. Influence of Sn doping ratio on the structural and optical properties of CdO films prepared by laser induced plasma. *Iraqi Journal of Physics*, 2020, vol. 18, no. 45, pp. 1–8. <https://doi.org/10.30723/ijp.v18i45.523>
22. Lober R., Mazumder J. Spectroscopic diagnostics of plasma during laser processing of aluminium // *Journal of Physics D: Applied Physics*. 2007. V. 40. N 19. P. 5917. <https://doi.org/10.1088/0022-3727/40/19/021>
23. Shehab M.M., Aadim K.A. Spectroscopic diagnosis of the CdO: CoO plasma produced by Nd:YAG laser // *Iraqi Journal of Science*. 2021. V. 62. N 9. P. 2948–2955. <https://doi.org/10.24996/ijis.2021.62.9.11>
24. Кисон В.Э., Мустафаев А.С., Сухомлинов В.С. Разработка новой плазменной технологии получения чистого белого корунда // Научно-технический вестник информационных технологий, механики и оптики. 2021. Т. 21. № 3. С. 380–385. <https://doi.org/10.17586/2226-1494-2021-21-3-380-385>
25. Aadim K.A., Ahmed B.M., Khalaf M.A. Influence of Sn doping ratio on the structural and optical properties of CdO films prepared by laser induced plasma // *Iraqi Journal of Physics*. 2020. V. 18. N 45. P. 1–8. <https://doi.org/10.30723/ijp.v18i45.523>

Authors

Mohammed Hamza Jawad — PhD Student, University of Baghdad, Baghdad, 00964, Iraq, [sc 58536603200](https://orcid.org/0009-0001-8111-8195), <https://orcid.org/0009-0001-8111-8195>, mohammed.hamza1204a@sc.uobaghdad.edu.iq

Mohammed Ridha Abdulameer — PhD, Professor, University of Baghdad, Baghdad, 00964, Iraq, [sc 56971327800](https://orcid.org/0000-0002-7395-9840), <https://orcid.org/0000-0002-7395-9840>, mohammed_plasma@sc.uobaghdad.edu.iq

Kadhim Abdulwahid Aadim — PhD, Professor, University of Baghdad, Baghdad, 00964, Iraq, [sc 56728936300](https://orcid.org/0000-0003-4533-5309), <https://orcid.org/0000-0003-4533-5309>, kadhim.aadim@ilps.uobaghdad.edu.iq

Received 18.03.2025

Approved after reviewing 21.06.2025

Accepted 23.07.2025

Авторы

Джавад Мохаммед Хамза — аспирант, Университет Багдада, Багдад, 00964, Ирак, [sc 58536603200](https://orcid.org/0009-0001-8111-8195), <https://orcid.org/0009-0001-8111-8195>, mohammed.hamza1204a@sc.uobaghdad.edu.iq

Абдуламир Мохаммед Ридха — PhD, профессор, Университет Багдада, Багдад, 00964, Ирак, [sc 56971327800](https://orcid.org/0000-0002-7395-9840), <https://orcid.org/0000-0002-7395-9840>, Mohammed_plasma@sc.uobaghdad.edu.iq

Аадим Кадхим Абдулвахид — PhD, профессор, Университет Багдада, Багдад, 00964, Ирак, [sc 56728936300](https://orcid.org/0000-0003-4533-5309), <https://orcid.org/0000-0003-4533-5309>, kadhim.aadim@ilps.uobaghdad.edu.iq

Статья поступила в редакцию 18.03.2025

Одобрена после рецензирования 21.06.2025

Принята к печати 23.07.2025



Работа доступна по лицензии
Creative Commons
«Attribution-NonCommercial»